iomac
International Operational Modal Analysis Conference

11th International Operational Modal Analysis Conference

20 - 23 May 2025 | Rennes, France

Quantification of errors in frequency-domain inverse force estimation due to measurement noise

Christof Van Zijl [1], *Jovana Jovanova*[2], *and Apostolos Grammatikopoulos* [3]

[1] Delft University of Technology, C.M.vanZijl@tudelft.nl
[2] Delft University of Technology, J.Jovanova@tudelft.nl
[3] Delft University of Technology, A.Grammatikopoulos@tudelft.nl

ABSTRACT
Inverse methods can be used to estimate wave excitation forces on offshore structures from measured dynamic responses, such as accelerations. Force estimation is particularly challenging at low frequencies, where offshore structures are typically excited by waves and where the frequency response function (FRF) is ill-conditioned, leading to amplification of measurement noise. This study investigates how measurement noise propagates into the estimated forces and examines the effectiveness of Tikhonov regularization in mitigating this effect. Theoretical expressions for the variance of the force estimates are derived, demonstrating that measurement noise results in error amplification proportional to the inverse FRF, producing large estimation errors at low frequencies. Regularization is introduced to reduce variance, but it also introduces bias to the estimated force. Constant and frequency-dependent regularization strategies are investigated. The trade-off between variance and bias is investigated, showing that while regularization stabilizes the inverse problem, it can introduce significant distortions in the estimated force spectrum, particularly at low frequencies. Since offshore structures are often loaded by waves with low frequencies, these findings underscore the importance of carefully selecting regularization parameters when applying inverse force estimation techniques to marine structures.

Keywords: frequency domain, inverse force, Tikhonov regularisation, uncertainty quantification

1. INTRODUCTION

Accurate knowledge of wave forces enable engineers to design marine structures that can withstand the harsh ocean environment, while simultaneously optimizing the performance and efficiency of these structures. In the shipping industry, wave force estimates can enable safe and efficient route planning [1], fuel optimization [2], and the development of autonomous ships [3].

Simulations used to predict the response of marine structures often focus on stationary behaviour over a wide range of operating conditions [4, 5]. These simulations typically involve harmonic analysis, where structural responses are predicted over a spectrum of wave frequencies. In such cases, the frequency domain offers an efficient framework for analysing the system's behaviour using the frequency response function (FRF). However, uncertainties in hydrodynamic models make it challenging to ensure that simulated wave forces accurately reflect real operating conditions [6]. Moreover, wave forces are difficult or impossible to measurement directly. Therefore, inverse methods provide an alternative solution, where measured responses (e.g. accelerations) can be used to estimate the forces acting on the structure [7].

A well-known challenge in force estimation is that the process is highly sensitive to errors in the frequency response function and measurement noise. This sensitivity arises because the frequency response function is often ill-conditioned, meaning small errors in the input measurements or system model can lead to large deviations in the estimated forces. Since ships and offshore structures are often loaded by low frequency wave excitation ($<<$ 1 Hz) [2], this ill-conditioning presents a major challenge for inverse force estimation in marine environments.

To address this, we first analyze how random measurement errors propagate into the estimated forces, deriving theoretical expressions for variance. We then investigate how regularization techniques, such as Tikhonov regularization, can mitigate ill-conditioning at low frequencies and reduce the uncertainty in force estimates. Finally, we assess the effectiveness of these techniques in the context of wave force estimation for large marine structures, where low-frequency excitation makes inverse methods particularly challenging.

2. THEORY

2.1. Frequency response function (FRF) forward model

Let $\underline{\mathbf{x}}(t) \in \mathbf{R}^n$ represent the responses of a n degree of freedom structure under the action of m input forces, $\underline{\mathbf{f}}(t) \in \mathbf{R}^n$. The equation of motion in the frequency domain is:

$$\begin{pmatrix} X_1(\omega) \\ X_2(\omega) \\ \vdots \\ X_n(\omega) \end{pmatrix} = \begin{pmatrix} H_{11}(\omega) & H_{12}(\omega) & \cdots & H_{1m}(\omega) \\ H_{21}(\omega) & H_{22}(\omega) & \cdots & H_{2m}(\omega) \\ \vdots & \vdots & \vdots & \vdots \\ H_{n1}(\omega) & H_{n2}(\omega) & \cdots & H_{nm}(\omega) \end{pmatrix} \begin{pmatrix} F_1(\omega) \\ F_2(\omega) \\ \vdots \\ F_m(\omega) \end{pmatrix} \implies \underline{\mathbf{X}}(\omega) = [\mathbf{H}]\, \underline{\mathbf{F}}(\omega) \tag{1}$$

Where $\underline{\mathbf{X}}(\omega) \in \mathbf{C}^n$ and $\underline{\mathbf{F}}(\omega) \in \mathbf{C}^n$ are the response and force vector in the frequency domain. $[\mathbf{H}](\omega) \in \mathbf{C}^{n \times m}$ is the frequency response function (FRF) matrix, which characterizes how forces are transmitted through the structure.

2.2. Inverse solution of the FRF forward model

The goal is to estimate the unknown force vector $\underline{\mathbf{F}}(\omega) \in \mathbf{C}^n$ from measured responses. However, in practice, measurements are noisy and the model must be modified to account for this uncertainty. Therefore, the forward model can be rewritten as follows [8]:

$$\underline{\hat{\mathbf{X}}} = [\mathbf{H}]\underline{\mathbf{F}} + \underline{\mathcal{E}} \tag{2}$$

Where $\underline{\hat{\mathbf{X}}}$ represents the noisy measurements and $\underline{\mathcal{E}} \in \mathbf{C}^n$ represents the measurement noise. If the noise in the time domain, $\underline{\varepsilon}$ is assumed to be a zero-mean Gaussian process with some variance, $[\mathbf{\Sigma_x}]$, applying the Discrete Fourier Transform (DFT) preserves its Gaussian nature:

$$\underline{\mathcal{E}} \sim \mathcal{N}(\underline{\mathbf{0}}, [\mathbf{\Sigma_X}]), \tag{3}$$

Where,

$$[\mathbf{\Sigma_X}] = \begin{cases} \frac{2}{N}[\mathbf{\Sigma_x}], & \text{if } k = 0, \\ \frac{4}{N}[\mathbf{\Sigma_x}], & \text{if } k = 1, 2, \ldots, N/2 + 1. \end{cases} \tag{4}$$

The factor N arises from scaling of the DFT (depending on its definition) while the factor of 2 accounts for the complex-valued frequency-domain signal. An additional factor of 2 for positive frequencies adjusts for the single-sided spectrum. The assumption of Gaussian noise in the measurement error is widely used in applications such as Kalman filtering [9] and Bayesian estimation [8, 10].

2.2.1. Least squares inverse solution

A common approach to solve the problem in Eq. 2 is to minimize the squared error between the predicted and measured responses [11]:

$$\underline{\hat{\mathbf{F}}}_{LS} = \text{argmin}_{\underline{\mathbf{F}}} \left|\left| \underline{\hat{\mathbf{X}}} - [\mathbf{H}]\underline{\mathbf{F}} \right|\right|_2^2 \tag{5}$$

which has the following closed-form solution:

$$\underline{\hat{\mathbf{F}}}_{LS} = [\mathbf{G}]_{LS}\underline{\hat{\mathbf{X}}} \quad \text{where } [\mathbf{G}]_{LS} = ([\mathbf{H}]^H[\mathbf{H}])^{-1}[\mathbf{H}]^H \tag{6}$$

The function $[\mathbf{G}]_{LS}$ maps the noisy measurements to the estimated force, and is often called the pseudo-inverse of $[\mathbf{H}]$ [11]. Here we refer to $[\mathbf{G}]_{LS}$ as the inverse FRF. As will be shown in Section 2.3. and Section 3.1., the inverse FRF $[\mathbf{G}]_{LS}$ is ill-conditioned at certain frequencies, leading to a large variance in $\underline{\hat{\mathbf{F}}}_{LS}$.

2.2.2. Inverse solution using Tikhonov regularization

One way to mitigate the large variance in the least-squares force estimate $\underline{\hat{\mathbf{F}}}$, Tikhonov regularization introduces a penalty term to improve stability [12]:

$$\underline{\hat{\mathbf{F}}}_{\lambda} = [\mathbf{G}]_{\lambda}\underline{\hat{\mathbf{X}}} \quad \text{where } [\mathbf{G}]_{\lambda} = ([\mathbf{H}]^H[\mathbf{H}] + \lambda[\mathbf{I}])^{-1}[\mathbf{H}]^H \tag{7}$$

The inverse FRF, $[\mathbf{G}]_{\lambda}$ now includes a regularization parameter, λ.

2.3. Uncertainty in force estimates

Under the Gaussian noise assumption adopted in Section 2.2., the least squares and regularized force estimates are both Gaussian random variables.

2.3.1. *Uncertainty in least squares estimate*

The least squares estimate is a Gaussian random variable with mean, $\underline{\mu}_{\underline{\hat{\mathbf{F}}}_{LS}}$ and variance, $[\mathbf{\Sigma}_{\underline{\hat{\mathbf{F}}}_{\mathbf{LS}}}]$ given below:

$$\underline{\mu}_{\underline{\hat{\mathbf{F}}}_{LS}} = \mathbf{E}[\underline{\hat{\mathbf{F}}}_{LS}] = \underline{\mathbf{F}} \tag{8}$$

$$[\mathbf{\Sigma}_{\underline{\hat{\mathbf{F}}}_{\mathbf{LS}}}] = \mathbf{E}[\underline{\hat{\mathbf{F}}}_{LS}\,\underline{\hat{\mathbf{F}}}_{LS}^{H}] = [\mathbf{G}]_{LS}[\mathbf{\Sigma}_{\mathbf{X}}][\mathbf{G}]_{LS}^{H} \tag{9}$$

The result for $[\mathbf{\Sigma}_{\underline{\hat{\mathbf{F}}}_{\mathbf{LS}}}]$ is due to the linear transformation properties of Gaussian distributions. From Eq. 8 the least squares estimate is clearly unbiased ($b_{LS} = \mathbf{E}[\underline{\hat{\mathbf{F}}}_{LS}] - \underline{\mathbf{F}} = \underline{\mathbf{0}}$). However, if $[\mathbf{H}]$ is nearly singular, the inverse $[\mathbf{H}]^{H}[\mathbf{H}]$ is ill-conditioned, leading to a large variance in $\underline{\hat{\mathbf{F}}}_{LS}$.

2.3.2. *Uncertainty in estimate using Tikhonov regularization*

The regularized least squares estimate is a Gaussian random variable with mean, $\underline{\mu}_{\underline{\hat{\mathbf{F}}}_{\lambda}}$ and variance, $[\mathbf{\Sigma}_{\underline{\hat{\mathbf{F}}}_{\lambda}}]$ given below:

$$\underline{\mu}_{\underline{\hat{\mathbf{F}}}_{\lambda}} = \mathbf{E}[\underline{\hat{\mathbf{F}}}_{\lambda}] = \underline{\mathbf{F}} + \lambda^{-1}[\mathbf{H}]^{H}\underline{\mathbf{F}} \tag{10}$$

$$[\mathbf{\Sigma}_{\underline{\hat{\mathbf{F}}}_{\lambda}}] = \mathbf{E}[\underline{\hat{\mathbf{F}}}_{\lambda}\,\underline{\hat{\mathbf{F}}}_{\lambda}^{H}] = [\mathbf{G}]_{\lambda}[\mathbf{\Sigma}_{\mathbf{X}}][\mathbf{G}]_{\lambda}^{H} \tag{11}$$

The regularized least squares estimate is biased since $b_{\lambda} = \mathbf{E}[\underline{\hat{\mathbf{F}}}_{\lambda}] - \underline{\mathbf{F}} = \lambda^{-1}[\mathbf{H}]^{H}\underline{\mathbf{F}} \neq \underline{\mathbf{0}}$. However, the regularization parameter, λ can be used to enforce smoothness of the solution and reduce the variance. The trade-off is that variance is reduced at the cost of introducing a bias.

3. NUMERICAL SIMULATION

To validate and gain further insight into theoretical predictions from Section 2, we now apply these methods to a two-degree-of-freedom system in a simple numerical simulation. Figure 3 presents a two-degree-of-freedom (2DOF) system used in the numerical simulations. In the simulation, the force applied at the first degree of freedom has three periodic components and is given by:

$$f_1 = (100\sin(2\pi 0.1t) + 100\cos(2\pi 0.1t)) + 100\sin(2\pi 0.5t) + 100\cos(2\pi 1t)\ \text{N} \tag{12}$$

This means that the force spectrum should have three peaks at **0.1** Hz, **0.5** Hz, and **1** Hz, with amplitudes of ≈**141** N, **100** N, and **100** N, respectively. No force is applied at the second degree of freedom $f_2 = 0$ N. The measured acceleration responses $\hat{x}_1$ and $\hat{x}_2$ include additive Gaussian noise, modeled based on a signal-to-noise ratio of 20 dB. The noise covariance, $[\mathbf{\Sigma}]_{\mathbf{x}}$ is then computed as:

$$[\mathbf{\Sigma}]_{\mathbf{x}} = \frac{1}{10^{SNR/10}}\begin{pmatrix}\text{Var}(x_1) & 0\\ 0 & \text{Var}(x_2)\end{pmatrix} \tag{13}$$

The aim is to estimate the unknown external forces acting on the system using the measured accelerations.

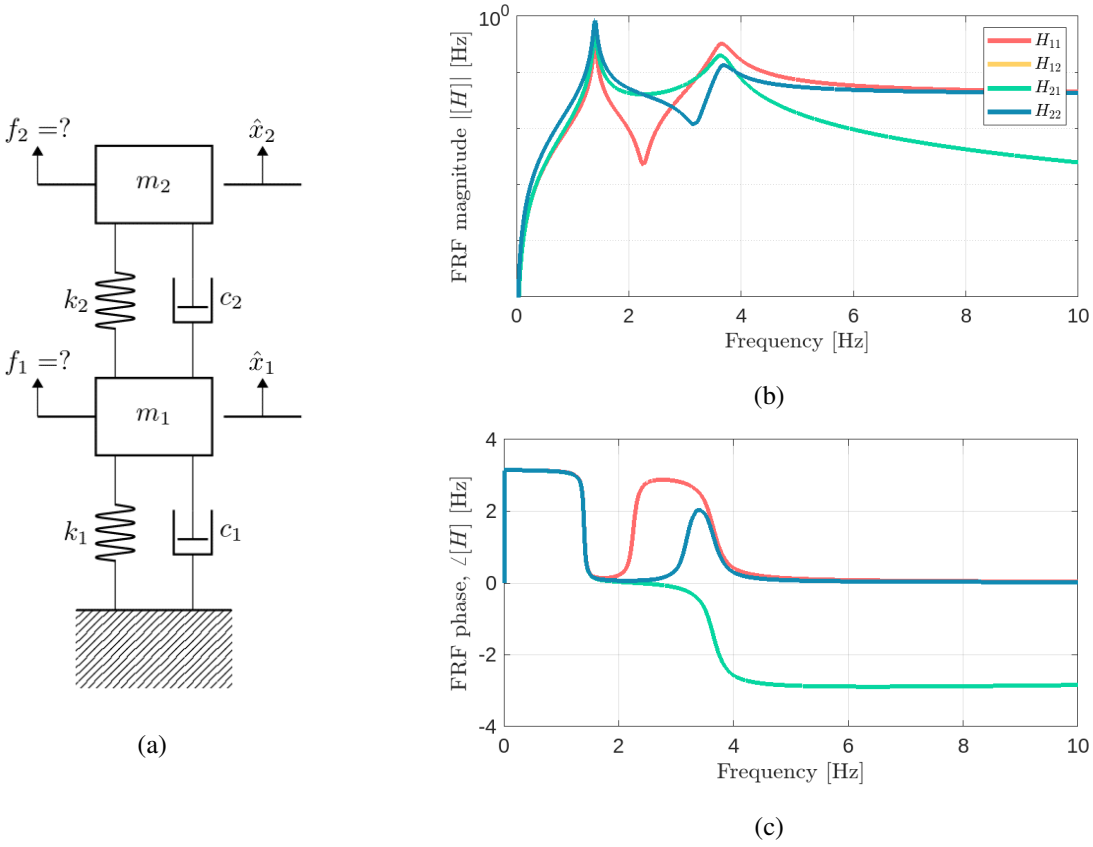

Figure 1: (a) Schematic of the two degree of freedom system setup used in numerical simulations with $m_1 = m_2 = 25$ kg, $k_1 = k_2 = 5000$ N/m, $c_1 = c_2 = 20$ N.s/m. (b) magnitude and (c) phase of the 2DOF system's FRFs. Two resonant peaks can clearly be identified, which correspond to the natural frequencies, $f_{n1} = 1.39$ Hz and $f_{n2} = 3.64$ Hz.

3.1. Effect of regularization on inverse solution

In Section 2.3. theoretical expressions for the variance of the estimated forces were derived for both the least-squares and regularized solutions. To gain further insight into the effect of regularization, Figure 2 (a) shows the inverse FRF $[\mathbf{G}]_{LS}$ and $[\mathbf{G}]_{\lambda}$ over a range of frequencies for different values of the regularization parameter. Similarly, Figure 2 (b) shows the variances in force estimates over the same frequencies and regularization parameters.

At low frequencies, the least-squares inverse FRF (i.e. $\lambda = 0$) has very high values, which leads to strong noise amplification. This is due to ill-conditioning of the inverse FRF matrix at low frequencies. In Figure 2 (b) this corresponds to extremely high variance in the force estimates at low frequencies. Regularization acts to flatten in the inverse FRF, reducing the sensitivity of the inverse problem to noise at these problematic frequencies. This can be seen in a reduction of the variance for the regularized estimates in Figure 2 (b). However, this clearly introduces a bias in the inverse FRF at low frequencies, which in turn leads to biased force estimates. In particular, regularization introduces unexpected peaks at certain frequencies in the inverse FRF, which can lead to spurious frequencies in the force estimates. The least-squares and regularized solutions are generally more similar at higher frequencies where the inverse FRF is more numerically stable. Moreover, dips in the variance curves for higher λ in Figure 2 (b) corresponds to the system's natural frequencies (1.4 Hz and 3.6 Hz), which shows that variance reduction is most pronounced at these frequencies.

Since the trade-off between bias and variance is frequency-dependent, a superior approach may be to a frequency-dependent regularization parameter. For example, λ may be chosen based on the properties of the FRF:

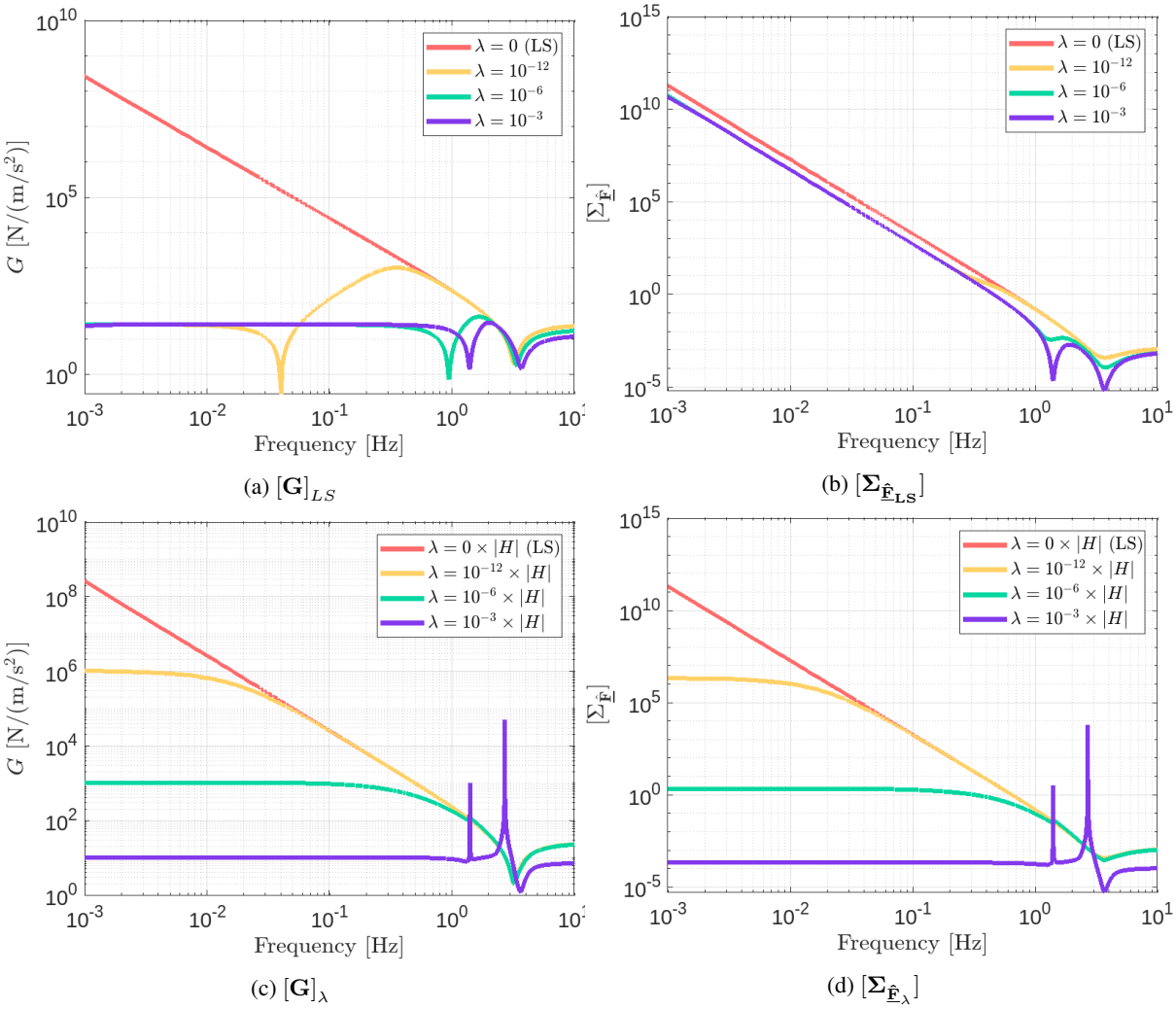

(a) $[\mathbf{G}]_{LS}$ (b) $[\mathbf{\Sigma}_{\hat{\mathbf{F}}_{\mathbf{LS}}}]$

(c) $[\mathbf{G}]_{\lambda}$ (d) $[\mathbf{\Sigma}_{\hat{\mathbf{F}}_{\lambda}}]$

Figure 2: Inverse FRF for least-squares compared to (a) constant λ and (c) frequency-dependent λ over a range of frequencies for different values of the regularization parameter. Variances in force estimates over the same frequencies and regularization parameters for (b) constant λ and (d) frequency-dependent λ.

$$\lambda(\omega) = \alpha \, |[\mathbf{H}(\omega]| \tag{14}$$

where α is a constant tuning parameter and $|[\mathbf{H}(\omega]|$ is the magnitude of the FRF matrix. Figure 2 (c) and (d) demonstrate the effect of a frequency-dependent regularization parameter on the inverse FRF and variance in force estimates, respectively. The frequency-dependent regularization exhibits some unexpected results:

- The variance in the estimated forces is lower at low frequencies compared to the least squares solution and solutions using a constant λ, despite prescribing less regularization where the FRF is small (i.e. at low frequencies). This is counterintuitive, as we would expect the variance to remain high in the low-frequency range when regularization is weak.
- The inverse FRF remains closer to the LS solution at low frequencies, suggesting that bias is also lower than in the constant case. Given that regularization is supposedly weaker at these frequencies, the expectation was that the bias behavior would resemble that of the unregularized case, yet we observe a notable bias.

The exact reason for these observations is unknown and further investigation is required to explain these results. Another important observation is that very large bias is generally introduced at low frequencies (< 1 Hz) using the frequency-dependent λ. This is an important consideration for marine structures, which often encounter waves with frequencies below 1 Hz.

3.2. Uncertainty in force estimates

To assess the effect of regularization on force estimation, Figure 3 presents the estimated forces in the frequency domain for four solution methods: the least-squares (LS) solution, constant regularization with $\lambda = 10^{-6}$, and frequency-dependent regularization with $\lambda = \alpha|H|$ for $\alpha = 10^{-6}$ and $\alpha = 10^{-3}$. Table 1 compares the true periodic components of the input force (at degree of freedom 1) with estimates obtained using each solution method, while Table 2 summarizes the root-mean-square error (RMSE) across all frequencies for each solution method. The following observations can be made:

- The constant $\lambda = 10^{-6}$ case has an almost negligible effect on noise compared to the LS case, with the RMSE for both $\hat{F}_1$ and $\hat{F}_2$ remaining ≈ 1.3 N (see Table 2). However, a significant bias of ≈ 40 N is introduced in $\hat{F}_1$ at $f_{e2} = 0.5$ Hz.
- The frequency-dependent λ is generally more effective at reducing variance than a constant λ, achieving an RMSE reduction of up to 97 % (from 1.3 N to 0.034 N for $\hat{F}_1$ and 0.027 N for $\hat{F}_2$). However, the variance at the excitation frequencies (f_{e1}, f_{e2}, and f_{e3}) remains comparable to the LS and constant λ cases, ≈ 12 N.
- Excessive regularization results in significant bias, particularly with frequency-dependent λ at $\alpha = 10^{-3}$, where bias exceeds 92% at $f_{e1} = 0.1$ Hz.
- Regularization, particularly in the frequency-dependent case, introduces spurious frequency components in the force estimate $\hat{F}_2$ (see Figure 3(d) and (h)).

λ	$\hat{F}_1$ [N]					
	$f_{e1} = 0.1$ Hz		$f_{e2} = 0.5$ Hz		$f_{e3} = 1$ Hz	
	μ	σ	μ	σ	μ	σ
True	141	n/a	100	n/a	100	n/a
0 (LS)	148	12.2	100	10.0	100	10.0
10^{-6}	142	12.0	60.4	7.78	97.4	9.87
$10^{-6} \times \|H\|$	144	12.1	100	10.0	100	10.0
$10^{-3} \times \|H\|$	9.92	3.16	55.1	7.42	84.2	9.08

Table 1: Empirical mean, μ and standard deviation, σ for three periodic components of $\hat{F}_1$ using different values of λ.

λ	**RMSE** $\times 10^4$ [N]	
	$\hat{F}_1$	$\hat{F}_2$
0 (LS)	1.4	1.3
10^{-6}	1.3	1.3
$10^{-6} \times \|H\|$	0.034	0.027
$10^{-3} \times \|H\|$	0.099	0.0016

Table 2: Root-mean-square error (RMSE) for $\hat{F}_1$ and $\hat{F}_2$ using different values of λ.

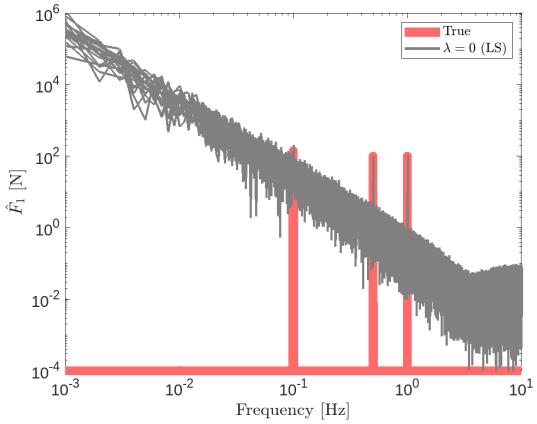

(a) Constant $\lambda = 0$ (LS)

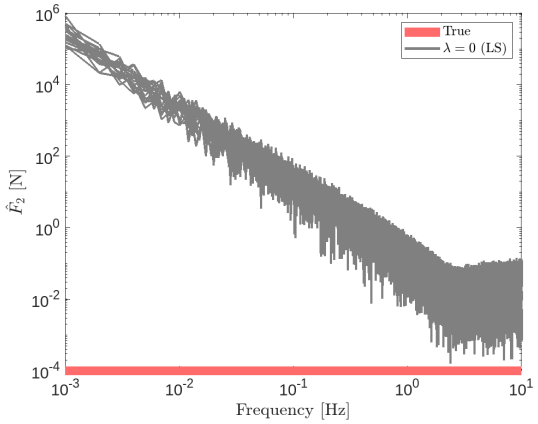

(b) Constant $\lambda = 0$ (LS)

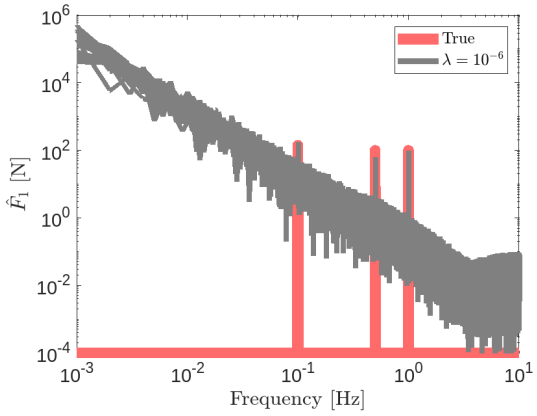

(c) Constant $\lambda = 10^{-6}$

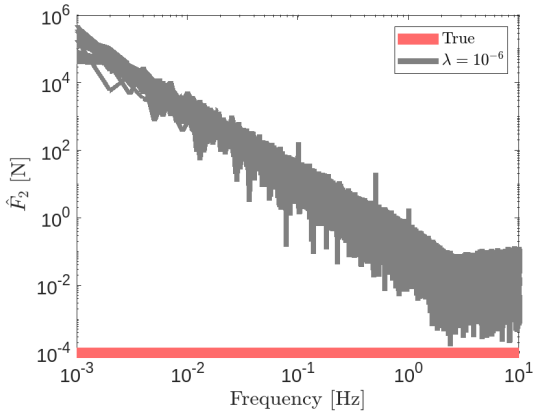

(d) Constant $\lambda = 10^{-6}$

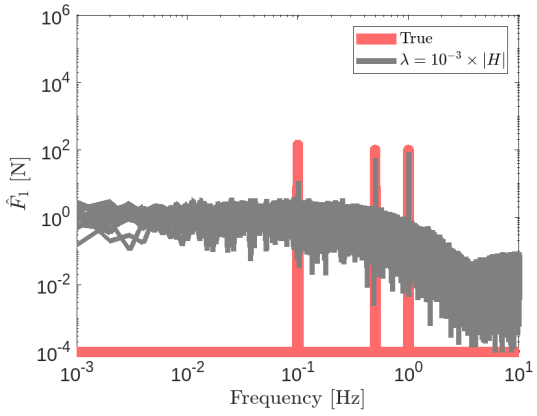

(e) Frequency-dependent $\lambda = 10^{-6} \times |H|$

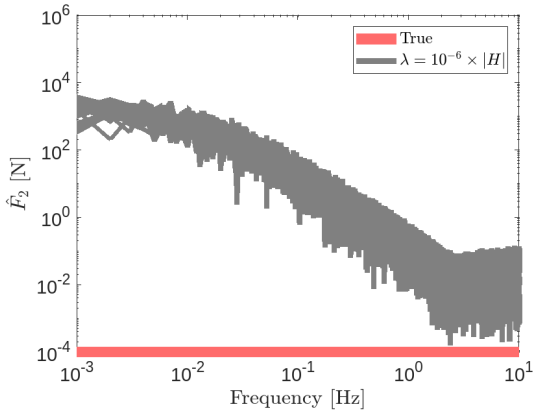

(f) Frequency-dependent $\lambda = 10^{-6} \times |H|$

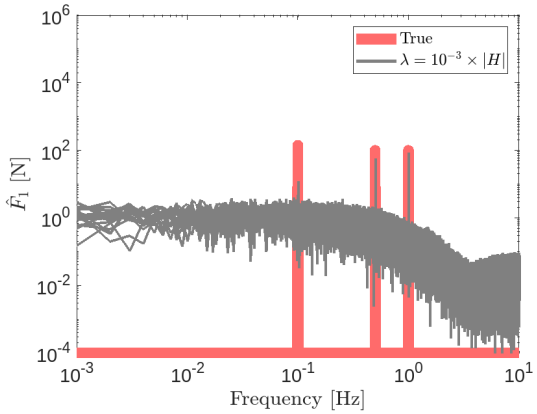

(g) Frequency-dependent $\lambda = 10^{-3} \times |H|$

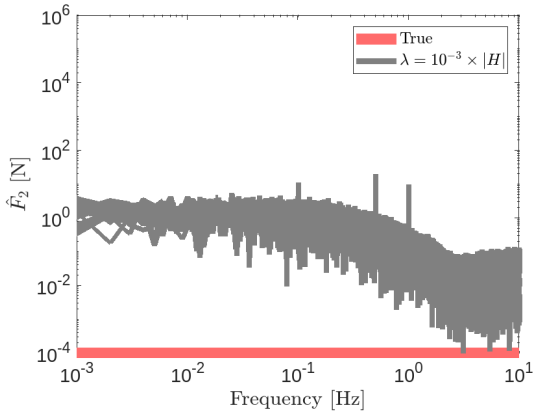

(h) Frequency-dependent $\lambda = 10^{-3} \times |H|$

Figure 3: The plots on the left show frequency-domain force estimates for degree of freedom 1, $\hat{F}_1$ for the LS solution and different values of λ. The true force has three periodic components at 0.1 Hz, 0.5 Hz, and 1 Hz. The plots on the right are for $\hat{F}_2$, which is zero at all frequencies.

4. CONCLUSIONS

This study demonstrates that inverse force estimation for ships and offshore structures is fundamentally limited by noise amplification due to the ill-conditioning of the FRF at low frequencies. Regularization techniques, particularly frequency-dependent Tikhonov regularization, significantly reduce variance at these frequencies but introduce bias and spurious frequency components. Although regularization improves numerical stability, it can distort the estimated force spectrum, which can affect its usefulness in fatigue analysis, route optimization, and structural health monitoring.

Given these challenges, alternative approaches may be necessary to improve force estimation in marine structures. These include, for example, exploring different frequency-dependent regularization parameters or using the time-domain Kalman filter. Future work should explore strategies to achieve a better balance between noise suppression and force accuracy, ensuring reliable force identification for fatigue analysis and structural health monitoring.

REFERENCES

[1] Lajic Z. Jensen J.J. Nielsen, U.D. Towards fault-tolerant decision support systems for ship operator guidance. *Reliability Engineering System Safety*, 104:1–14, 2024.

[2] Bingham H.B. Brodtkorb A.H. et al. Nielsen, U.D. Estimating waves via measured ship responses. *Scientific Reports*, 13(17342), 2023.

[3] Bridgelall R. Abudu, R. Autonomous ships: A thematic review. *World*, 5(2):276–292, 2024.

[4] Temarel P. Hirdaris, S.E. Hydroelasticity of ships: Recent advances and future trends. *Proceedings of the Institution of Mechanical Engineers, Part M: Journal of Engineering for the Maritime Environment*, 223(3), 2009.

[5] Alley A. Brandt A. et al. Ergin, A. Committee i.2: Dynamic response. In *International Ship and Offshore Structures Congress*, 2018.

[6] Bai W. de Hauteclocque G. et al. Ogawa, Y. Committee i.2: Loads. In *International Ship and Offshore Structures Congress*, 2018.

[7] Øiseth O. Lourens E. Petersen, Ø.W. Full-scale identification of the wave forces exerted on a floating bridge using inverse methods and directional wave spectrum estimation. *Mechanical Systems and Signal Processing*, 120(1):708–726, 2019.

[8] M. Aucejo and O. De Smet. On a full bayesian inference for force reconstruction problems. *Mechanical Systems and Signal Processing*, 104(1):36–59, 2018.

[9] Reynders E. De Roeck G. Degrande G. Lourens, E. and G. Lombaert. An augmented kalman filter for force identification in structural dynamics. *Mechanical Systems and Signal Processing*, 27(1): 446–460, 2012.

[10] M. Aucejo and O. De Smet. An optimal bayesian regularization for force reconstruction problems. *Mechanical Systems and Signal Processing*, 126(1):98–115, 2019.

[11] Rolfes R. Jonkman J. Pahn, T. Inverse load calculation procedure for offshore wind turbines and application to a 5-mw wind turbine support structure. *Wind Energy*, 20(1):1171–1186, 2017.

[12] P.C. Hansen. Regularization tools: A matlab package for analysis and solution of discrete ill-posed problems. *Numerical Algorithms*, 6(1):1–35, 1994.